



Note

A luminescent Pt-POCN pincer complex via direct cyclometalation



Kevin B. Lavelle, Liliana Gutierrez, Jeanette A. Krause, William B. Connick*

University of Cincinnati, Department of Chemistry, PO Box 210172, Cincinnati, OH 45221-0172, USA

ARTICLE INFO

Article history:

Received 19 December 2014

Received in revised form

1 March 2015

Accepted 3 March 2015

Available online 11 March 2015

Keywords:

Cyclometalation

Platinum

Mixed-donor

Pincer complex

Crystal structure

Emission spectroscopy

ABSTRACT

We report the synthesis of the novel pincer complex $\kappa^P, \kappa^C, \kappa^N$ -[2,6-(iPr)₂PO)-(C₆H₃)(CH₂[c-N(CH₂)₄O])]PtBr (Pt(POCN)Br, **1a**) by direct cyclometalation of PtBr₂(SEt₂)₂. This represents the first report of a mixed-donor platinum pincer complex synthesized using cyclometalation. The complex is emissive in the solid state and frozen solution. Comparison of the structure of **1a** to related pincer complexes provides insights into the effect of pincer arm donor substituents on cyclometalation.

© 2015 Elsevier B.V. All rights reserved.

Introduction

For a number of years, chelating symmetric pincer complexes of platinum group metals have been studied, with emphasis on catalytic applications [1–6]. For example, phosphine and phosphinite pincer complexes are active catalysts for reactions ranging from CO₂ reduction [7–9], hydrosilylation [10,11], and the Kharasch addition [12] to organic carbon–carbon coupling reactions [13]. More recently, there has been growing interest in mixed-donor ligands, in which either the central carbon donor is replaced with a heteroatom [14–16] or the two pincer arms each have different donors [17–20]. These modifications influence the ligand's steric and donor properties, allowing for fine-tuning of reactivity (Scheme 1). Less attention has been given to their electronic and emission spectroscopic properties. Even among symmetric pincer ligand complexes, although NCN derivatives have been the subject of a number of such studies [21–31] (e.g., Pt(pip₂NCN)Lⁿ⁺ complexes [29], Scheme 1), phosphorus-containing pincer complexes have received comparatively little attention. One exception is the work of Zargarian and coworkers, which focused on a charge-transfer band observed at approximately 400 nm in both nickel POCOP and POCN complexes. The effects of modifications to pincer ligand substituents, metal oxidation state, and trans-ligand were

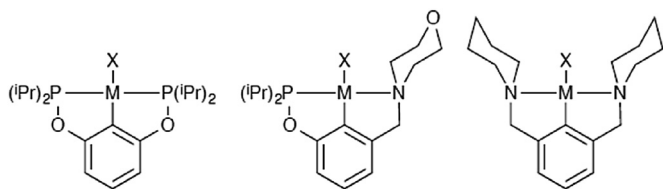
examined [12,17,32,33]. Such studies have served to deepen understanding of the influence of ligand architecture on the electronic structures of pincer complexes, which is essential for intelligent ligand design aimed at accessing multielectron catalytic properties of pincer complexes using light.

Because of the rich emission spectroscopy, long-lived excited states and photochemistry of many platinum complexes, there is particular interest in mixed-donor pincer ligand platinum complexes. Yet surprisingly little precedent exists for the synthesis of such compounds. The one platinum POCN complex previously reported was synthesized via oxidative addition [19]. However, that synthetic route requires use of a Pt⁰ precursor that is prepared in low yield [34,35]. In a second strategy, lithiation of a brominated metal precursor has proven a reliable choice for synthesis of NCN complexes [36]. However, that route is problematic for synthesis of phosphinite complexes, because attack on the P–O bond by nucleophilic organolithium reagents competes with the desired metal-halide substitution chemistry. Another possible strategy is trans-cyclometalation, which takes advantage of the relative strength of Pt–P bonds vs. Pt–N bonds to accomplish the formal exchange of ligands, such as replacement of an NCN ligand with a PCP ligand [37]. An inconvenience of this approach is the need to prepare a cyclometalated starting material.

An attractive alternative route is direct cyclometalation, which has been employed successfully with platinum phosphine pincer complexes since the earliest days of pincer complex chemistry [38] and has been used previously in preparation of platinum

* Corresponding author.

E-mail address: william.connick@uc.edu (W.B. Connick).



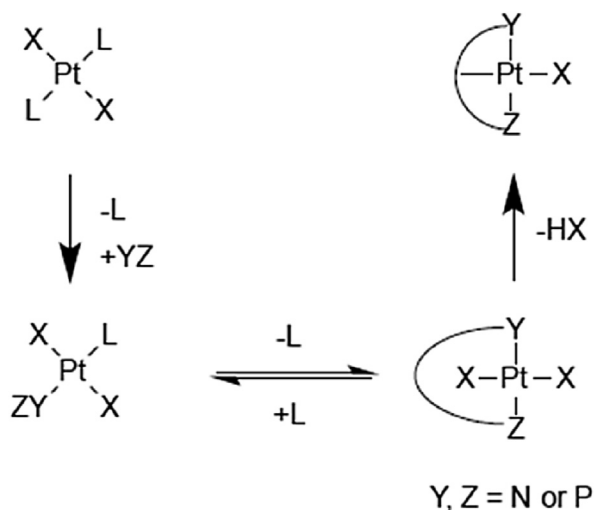
Scheme 1. Types of pincer complexes.

phosphinite pincer complexes [39]. One possible mechanism involves coordination of the pincer arms prior to C–H activation, as shown in Scheme 2; other mechanisms are possible, including those in which an amine pincer arm acts as an internal base [37]. In the case of cyclometalation, care must be taken in choice of metal precursor in order to circumvent formation of insoluble Pt^{II} and Pd^{II} oligomers [38,40,41]. Moreover, direct cyclometalation has a mixed record with respect to platinum NCN-type pincer complexes and is typically not a practical synthetic route. For example, this is not an effective approach for the synthesis of Pt(pip₂NCN)Br and related complexes [29]. Studies suggest that the bonds between the metal and aliphatic amines of the pincer arms are comparatively weak. Therefore, it is more difficult to achieve simultaneous coordination of both pincer arms, which for the mechanism shown in Scheme 2, is believed to be necessary to promote activation of the relatively inert central *sp*² C–H bond [1]. Herein, we examine the intermediate case involving a mixed-donor pincer ligand. Whereas a previous synthesis of platinum POCN-type pincer complexes has been accomplished via the oxidative addition route [19], here we report the preparation of a novel mixed-donor platinum pincer complex, Pt(POCN)Br, by direct cyclometalation (Scheme 1) of a dihalobis(thioether) platinum precursor. Analysis of the conditions under which this cyclometalation occurs, as well as comparison of the structure of Pt(POCN)Br with other known pincer complexes, provides insight into the influence of pincer arm substituents on cyclometalation.

Experimental

General

PtBr₂, NiBr₂, 3-hydroxybenzaldehyde, chlorodiisopropylphosphine, and ethyl sulfide were purchased from Sigma Aldrich. All other reagents were purchased from Fisher. Benzene was



Scheme 2. Steps during cyclometalation of pincer complexes.

purchased from Alfa Aesar, n-hexane was purchased from Tedia, ethyl acetate was purchased from Pharmco-Aaper, high-purity spectroscopic anhydrous methanol and ethanol were purchased from Sigma Aldrich, and all other solvents were purchased from Fisher. THF was distilled after drying over sodium metal and benzophenone. Toluene and benzene were dried over calcium hydride and distilled prior to use. Air-sensitive work was performed under an argon atmosphere using standard Schlenk and glovebox techniques. Solvents for air-sensitive reactions were degassed using three freeze-pump-thaw cycles. PtBr₂(SEt₂)₂ was prepared analogously to a literature procedure for the preparation of PtCl₂(SEt₂)₂ [42].

¹H and ³¹P NMR spectra were recorded at room temperature using a Bruker AC 400 MHz instrument. Deuterated solvents (CDCl₃ and C₆D₆) were purchased from Cambridge Isotope Laboratories. ¹H NMR spectra are reported relative to TMS, and ³¹P NMR spectra are reported relative to 85% H₃PO₄ at δ = 0. UV–visible absorption spectra were recorded using a HP8453 UV–visible diode array spectrometer. Frozen solution emission spectra were recorded using a SPEX Fluorolog-3 fluorimeter equipped with a double-emission monochromator and a single excitation monochromator. 77 K Glassy solutions were prepared by inserting a quartz EPR tube containing a 4:1 ethanol:methanol solution of the respective complex into a quartz-tipped finger dewar. Emission spectra were corrected for instrumental response. Solid-state emission spectra were collected using a Renishaw Raman Microscope using a 442 nm HeCd laser for excitation and a 20x objective lens to magnify the sample. Mass spectra were obtained by electrospray ionization (ESI) of acetonitrile solutions using a Micromass Q-TOF-2 instrument.

Synthesis of Pt(POCN)Br (1a)

The ligand precursor, POC(H)N, was prepared *in situ*. To a solution of chlorodiisopropylphosphine (1.3 mmol, 0.21 mL) in 5 mL toluene was added via cannula a solution of 3-((morpholino)methyl)phenol (1.3 mmol, 0.3455 g) and triethylamine (1.6 mmol, 195 μL) in 5 mL toluene at 10 °C and allowed to warm to room temperature while stirring. The mixture was filtered to remove precipitate, and the solvent was removed to give a pale orange oil. Next, a 2 mL toluene solution of PtBr₂(S(CH₂CH₃)₂)₂ (1.3 mmol, 0.6796 g) and triethylamine (1.6 mmol, 195 μL) were added to POC(H)N via cannula, and the resulting solution was refluxed for 24 h. After cooling to room temperature, the solvent was removed under vacuum. The product was purified by chromatography using a silica column and dichloromethane as the eluent. Yield: 0.1231 g, 17%. ¹H NMR (CDCl₃, δ): 1.21–1.26 (dd, ³J_{PH} = 16 Hz, ³J_{HH} = 7 Hz, 6H, PCHCH₃), 1.32–1.39 (dd, ³J_{PH} = 19 Hz, ³J_{HH} = 7 Hz, 6H, PCHCH₃), 2.41–2.49 (m, 2H, PCH), 2.92 (d, ³J_{HH} = 13 Hz, 2H, NCH₂CH₂), 3.88–3.98 (m, 4H, ArCH₂N and OCH₂CH₂), 4.21 (t, ³J_{HH} = 11 Hz, 2H, NCH₂CH₂), 4.49 (t, ³J_{HH} = 12 Hz, OCH₂CH₂), 6.66 (d, ³J_{HH} = 8 Hz, 1H, {Ar}H⁵), 6.74 (d, ³J_{HH} = 7 Hz, 1H, {Ar}H³), 6.98 (t, ³J_{HH} = 8 Hz, 1H, {Ar}H⁴). ³¹P{¹H} NMR (CDCl₃, δ) 160.56 (J_{PP} = 4655 Hz). MS-ESI (m/z). Observed (Calculated): 582.1 (582.1), [Pt(POCN)BrH]⁺; 605.1 (605.1), [Pt(POCN)BrNa]⁺; 503.2 (503.1) [Pt(POCN)]⁺.

Synthesis of Ni(POCN)Br (1b)

The product was prepared by modification of the procedure of Zargarian et al. [17]; however, the metal precursor was added directly to the ligand precursor without first isolating the ligand precursor. A solution of chlorodiisopropylphosphine (2.7 mmol, 0.45 mL) in 7.5 mL THF was added via cannula to a solution of 3-((morpholino)methyl)phenol (2.6 mmol, 0.5046 g) and triethylamine (2.8 mmol, 400 μL) in 17.5 mL THF at –10 °C and allowed to

warm to room temperature while stirring. The mixture was filtered to remove precipitate, and the filtrate was evaporated to dryness to give a pale orange oil. A 20 mL benzene solution of NiBr₂ (2.7 mmol, 0.219 g) and triethylamine (2.8 mmol, 400 μL) were added via cannula, and the resulting solution was refluxed for 3 h. After cooling to room temperature, the reaction mixture was filtered through a plug of silica, and the filtrate was dried. Further purification was achieved by crystallization via slow diffusion of n-hexane into a saturated benzene solution of the product to give dark yellow/brown crystals. Yield: 0.7251 g, 63%. ¹H NMR (C₆D₆, δ): ¹H NMR (C₆D₆, δ): 1.16–1.21 (dd, ³J_{PH} = 15 Hz, ³J_{HH} = 7 Hz, 6H, PCHCH₃), 1.47–1.53 (dd, ³J_{PH} = 18 Hz, ³J_{HH} = 7 Hz, 6H, PCHCH₃), 2.19–2.28 (m, 2H, PCH), 2.34 (d, ³J_{HH} = 13 Hz, 2H, NCH₂CH₂), 3.17 (t, ³J_{HH} = 12 Hz, 2H OCH₂CH₂), 3.24 (d, ³J_{HH} = 12 Hz, 2H, NCH₂CH₂), 3.63 (s, 1H, ArCH₂N), 4.24 (t, ³J_{HH} = 12 Hz, OCH₂CH₂), 6.45 (d, ³J_{HH} = 7 Hz, 1H, {Ar}H⁵), 6.65 (d, ³J_{HH} = 8 Hz, 1H, {Ar}H³), 6.95 (t, ³J_{HH} = 8 Hz, 1H, {Ar}H⁴). ³¹P{¹H} NMR (C₆D₆, δ) 200.67. MS-ESI (m/z). Observed (Calculated): 445.0 (445.0), [Ni(POCN)Br]⁺.

X-ray crystallography

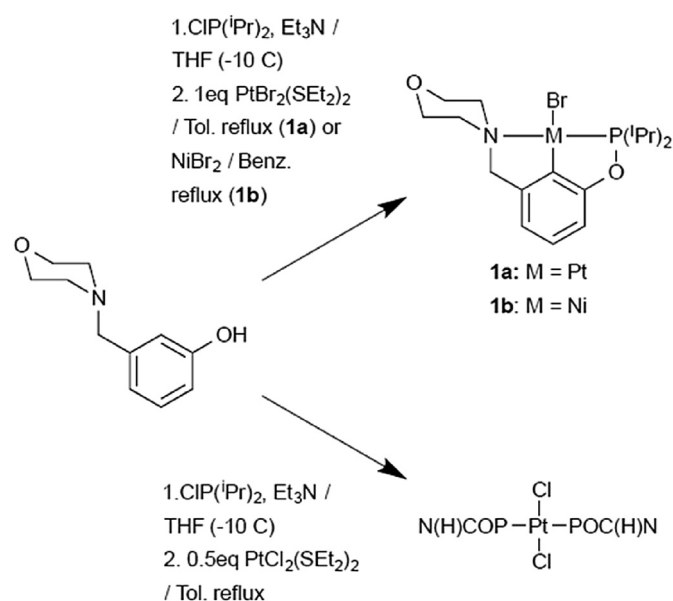
Colorless rod-shaped crystals of **1a** were grown by slow diffusion of n-hexane into a benzene solution. Yellow block-shaped crystals of Ni(POCN)Cl (**1c**) were grown by slow diffusion of n-hexane into saturated benzene solution. Air-sensitive colorless plate-shaped crystals of the chloride salt of the protonated brominated ligand precursor, [POC(Br)NH]Cl (**POC(Br)N**), were grown from diethyl ether (see Appendices for further information).

For X-ray examination, suitable crystals of **1a** and **1c** were each mounted in loops with Paratone-N oil and transferred to the goniostat bathed in a cold stream. Intensity data were collected at 150 K on a standard Bruker SMART6000 CCD diffractometer using graphite-monochromated Cu Kα radiation, λ = 1.54178 Å. The data frames were processed using the program SAINT. The data were corrected for decay, Lorentz and polarization effects as well as absorption and beam corrections based on the multi-scan technique. The structures were solved by a combination of direct methods in SHELXTL and the difference Fourier technique and refined by full-matrix least squares on F². Non-hydrogen atoms were refined with anisotropic displacement parameters. The positions of the H-atoms were calculated and treated with a riding model in subsequent refinements.

Results and discussion

Synthesis

The protonated phosphinite ligand precursor, POC(H)N, was prepared using the method developed by Zargarian et al. [17]. However, because this compound is susceptible to hydrolysis under atmospheric conditions, we found it convenient to keep its manipulation to a minimum and proceed immediately to the cyclometalation step (Scheme 3). Using NiBr₂, the cyclometalation reaction proceeds smoothly in refluxing benzene to give Ni(POCN)Br (**1b**) within 4 h. Ni(POCN)Cl (**1c**) was isolated from the reaction of **1b** with Pt(COD)Cl₂. By contrast, we saw no evidence of formation of a pincer complex under the same conditions using PtBr₂(SEt₂)₂. Also unsuccessful was an attempt to prepare the platinum pincer complex by lithiation of the brominated ligand precursor POC(Br)N using butyllithium followed by addition of the platinum precursor. On the other hand, refluxing POC(H)N in toluene with PtBr₂(SEt₂)₂ for a longer period of time (24 h) gave Pt(POCN)Br (**1a**) in good yield. This result indicates that, contrary to the typical NCN case, direct cyclometalation using POC(H)N is a perfectly practical synthetic route. Interpretation of these results in



Scheme 3. Synthesis of pincer complexes.

context of the mechanism in Scheme 2 suggests that the combination of phosphorus and aliphatic amine donor groups is sufficient for bonding of POC(H)N in a trans-bidentate fashion, which occurs prior to C–H bond activation. More broadly, application of Hammond's postulate to this case suggests a transition state that resembles the cyclometalation product. Because the Pt–P bond is stronger than the Pt–N bond, it follows that the barrier to C–H bond activation will be lower in the POCN case than in the NCN case by approximately the difference between the Pt–P and Pt–N bond energies. This prediction holds for Scheme 2, as well as other mechanisms in which the Pt–P bond forms prior to the transition state, including ones in which the morpholino group acts as an internal Brønsted base. We believe that this effect is a significant factor in the efficacy of cyclometalation with POC(H)N.

Interestingly, when the same reaction conditions with PtCl₂(SEt₂)₂ were employed in the presence of two equivalents of POC(H)N, very little pincer complex formed. Instead, as indicated by ¹H and ³¹P{¹H} NMR spectra, as well as mass spectrometry data, the reaction yielded a symmetric bis-pincer complex, Pt(η¹-POC(H)N)₂Cl₂, in which each POC(H)N ligand is bonded to Pt^{II} through phosphorus (Scheme 3). Notably, in CDCl₃ solution a single resonance was present in the ³¹P{¹H} NMR spectrum at 124 ppm with platinum satellites (J_{PtP} = 2666 Hz), confirming bonding of phosphorus to the metal. The ¹H NMR spectrum showed that the phosphinite methine proton resonances were shifted downfield, as expected for coordination to Pt(II), whereas the morpholine and aromatic resonances appear at chemical shifts more consistent with the free ligand precursor. The major peaks in the ESI mass spectrum were consistent with the singly and doubly protonated bis-pincer complexes, Pt(POCN)(POCNH)Cl₂⁺ and Pt(POCNH)₂Cl₂⁺, respectively. In contrast, Pt(η¹-POCN)₂Cl₂ is unstable in air and decomposed within 48 h, most likely via ligand hydrolysis. The bis-pincer product is reminiscent of insoluble oligomers {–PC(H)P–M–}_n proposed to form during cyclometalation reactions aimed at preparing Pt and Pd PCP complexes [38,40,41]. In the present case, strong Pt–P bonds (c.f., Pt–N bonds) and 2:1 ligand-to-metal ratio favor formation of the bis-POC(H)N complex (analogous to {–PCP–M–}_n oligomers), rather than a monomeric η³-pincer complex. Moreover, these results indicate that a pendant amine group is ineffective at displacing a trans-situated P-donor group of another

POC(H)N ligand, as would be required to occur prior to C–H activation ultimately leading to **1a** (Scheme 2).

Crystal structure

The structures of **1a** and **1c** were confirmed by X-ray crystallography (Fig. 1). The distances and angles are normal (Table 1), and there are no unusual intermolecular interactions. Little difference is observed between the structure of **1c** and that previously reported for **1b**, other than the Ni-halide bond lengths. In the case of the platinum complex, **1a**, the distance (4.302(5) Å) between pincer arm donor N and P atoms is intermediate between those of Pt(NCN)Cl (N = piperidine; 4.156(5) Å, 4.174(5) Å) [29] and Pt(POCOP)Cl (P = diisopropylphosphinite; 4.471(1) Å, 4.458(2) Å) [39], consistent with the relative lengths of Pt–P and Pt–N bonds. The P–Pt–N bond angle (159.44(14)°) is several degrees smaller than the P–Pt–P angles of Pt(POCOP)Cl (161.20(4)°; 160.79(4)°) [39] and the N–Pt–N angles of Pt(NCN)Cl (164.29(13)°, 164.75(14)°) [29]. Also, and in keeping with the relative trans influence of the phosphorus and nitrogen donor groups, the Pt–N bond is longer than in the NCN complex, and the Pt–P bond is shorter than in the POCOP complex (Table 2).

Interestingly, comparison of the structure of **1a** with that of the nickel analog **1b** provides insight into possible reasons for differing outcomes under cyclometalation conditions. In crystals of **1a**, there is greater deviation from ideal square planar coordination geometry as compared to the previously reported nickel analog, **1b** [17]. For example, the P–Pt–N bond angle (159.44(14)°) is significantly smaller than found for **1b** (162.20(6)°); this strain is attributable to longer metal–ligand bond lengths in the platinum complex (Table 1), in accord with the larger size of platinum. Through application of Hammond's postulate it may be suggested that increased strain in **1a** compared to **1b**, as evidenced by these deviations from ideal square planar geometry, will contribute to a higher activation energy for platinum cyclometalation as compared to nickel.

UV–visible absorption spectroscopy

In an effort to build on existing pincer complex electronic structure data, electronic spectra were collected for **1a** and for its nickel analog, **1b** (Fig. 2). At longer wavelengths (>300 nm), two

Table 1
Selected bond lengths (Å) and angles (°) for **1a** and **1b**.

Measurement	Pt(POCN)Br	Ni(POCN)Br[17]	Ni(POCN)Cl
M–C(1)	1.966(6)	1.853(2)	1.855(3)
M–P(1)	2.1802(15)	2.1107(6)	2.1140(8)
M–N(1)	2.192(5)	2.0428(18)	2.046(2)
M–X	2.5088(7)	2.3319(4)	2.2300(7)
C(1)–M–X	175.77(19)	176.26(7)	176.41(9)
P(1)–M–N(1)	159.44(14)	162.20(6)	161.54(7)
P(1)–M–X	99.86(5)	95.08(2)	96.00(3)
N(1)–M–X	97.48(13)	99.65(5)	98.93(7)
P(1)–M–C(1)	82.12(19)	81.72(7)	81.93(9)
N(1)–M–C(1)	79.9(2)	83.85(9)	83.67(11)

Table 2
Comparison of selected bond lengths and angles of platinum pincer complexes.

Structure	M–C (Å)	M–P (Å)	M–N (Å)
Pt(POCN)Br	1.966(6)	2.1802(15)	2.192(5)
Pt(NCN)Cl [29]	1.910(4); 1.899(5)	–	2.115(4); 2.101(4); 2.099(3); 2.094(3)
Pt(POCOP)Cl [39]	1.984(3); 1.976(4)	2.2688(10); 2.2619(11); 2.2592(10)	–
Structure	D–M–D (°)	D–M–C (°)	D–D (Å)
Pt(POCN)Br	159.44(14)	82.12(19) (P); 79.9(2) (N)	4.302(5)
Pt(NCN)Cl [29]	164.29(13); 164.75(14)	82.0(2); 82.3(2); 82.4(2); 82.5(2)	4.156(5); 4.174(5)
Pt(POCOP)Cl [39]	161.20(4); 160.79(4)	80.50(11); 80.72(11); 80.61(12); 80.55(12)	4.471(1); 4.458(2)

broad, moderately intense absorption bands occur in the spectrum of **1b** near 330 nm (5800 M^{−1} cm^{−1}) and 400 nm (1200 M^{−1} cm^{−1}). These apparent charge-transfer bands closely resemble those observed in absorption spectra of other nickel-phosphinite pincer complexes; a band corresponding to that observed at 400 nm in **1a** has typically been assigned to a MLCT transition [12,17,32,33]. The absorption spectrum of **1a** features a broad, moderately intense charge-transfer band at 293 nm (3400 M^{−1} cm^{−1}). Both the 293 and 330 nm bands in the spectrum of **1b** exhibit mild solvatochromism, characterized by a blue-shift with increasing polarity. A review of the literature pertaining to charge-transfer spectra of square planar d⁸-electron complexes generally [43–46], and with particular

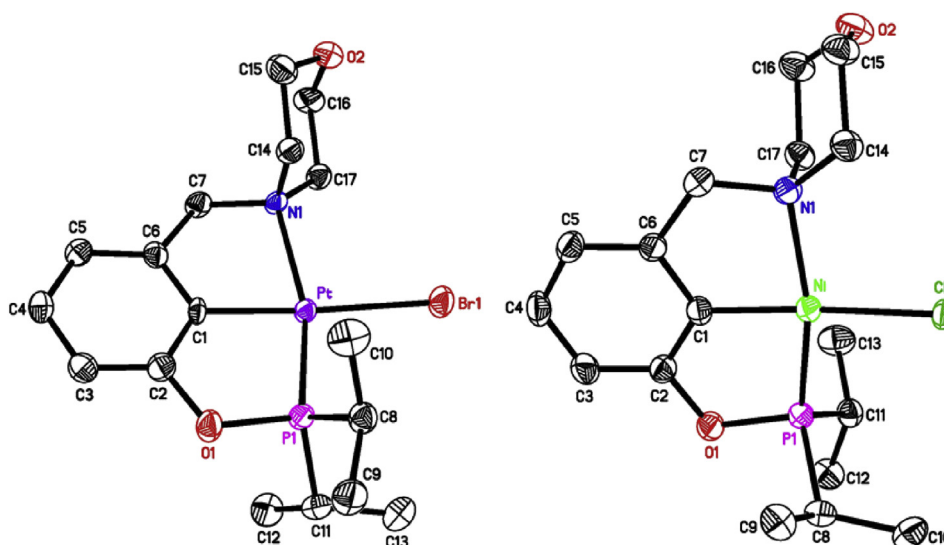


Fig. 1. ORTEP drawings of Pt(POCN)Br (**1a**, left) and Ni(POCN)Cl (**1c**, right), 50% probability ellipsoids. H- atoms omitted for clarity.

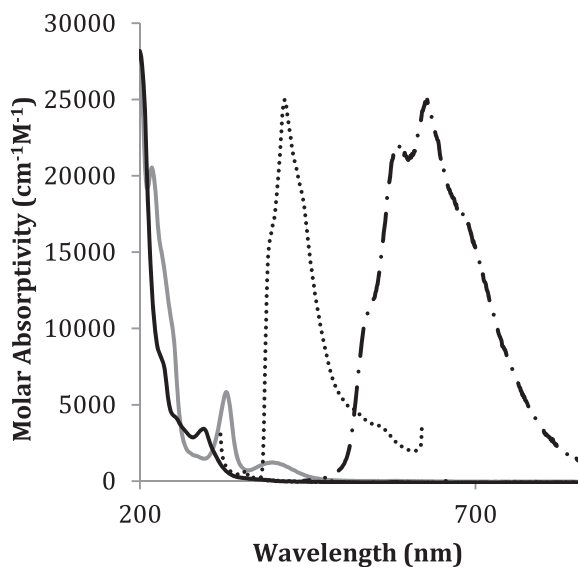


Fig. 2. UV-Visible absorption spectra for **1a** (black trace) and **1b** (gray trace), 77 K solid state emission spectrum for **1a** ($\lambda_{\text{ex}} = 314$ nm, dotted black trace), and 298 K solid state emission spectrum for **1a** ($\lambda_{\text{ex}} = 442$ nm, dashed black trace). Emission spectra are arbitrarily scaled.

emphasis on phosphinite pincer complexes [12,17,32,33], indicates that arguments can be made for either a halide-to-metal LMCT or a metal-to-phosphine MLCT assignment.

Emission spectroscopy

Whereas emission from the nickel analog is vanishingly weak, **1a** gives rise to two distinct emission bands. Room-temperature and 77 K solid-state, as well as dilute 77 K glassy solution (4:1 ethanol:methanol) emission spectra were recorded. For **1a**, two weakly structured emission bands were observed. The more intense 410 nm band is observed both in the solid-state and 77 K glassy solution ($\lambda_{\text{ex}} = 314$ nm). The weaker 570 nm band was observed only in the solid state ($\lambda_{\text{ex}} = 442$ nm), and presumably this emission is too weak to observe in dilute frozen solution. Both bands exhibit similar structure, with vibronic spacing of approximately 1200 cm^{-1} , consistent with aromatic ligand stretching modes. The similarity suggests that the longer wavelength emission arises from the triplet excited state, whereas the shorter wavelength emission arises from the corresponding singlet state.

Conclusions

The successful synthesis of a novel mixed-donor platinum POCN pincer complex using cyclometalating conditions obviates the need for poorly yielding syntheses of Pt^0 precursors. A contributing factor to the increased reactivity of the POC(H)N ligand precursor as compared to NC(H)N analogs is the difference between the Pt–P and Pt–N bond energies. Interestingly, in the presence of excess ligand, $\text{Pt}(\eta^1\text{-POCN})_2\text{Cl}_2$ was observed to form. Crystallographic data, as well as the observed formation of $\text{Pt}(\eta^1\text{-POCN})_2\text{Cl}_2$, suggest that the strength of the bonds between the metal center and the pincer donor arms influences which intermediate states are favored, and therefore, whether cyclometalation is favorable.

Acknowledgments

This research was supported by the National Science Foundation (CHE-1152853). Funding for the SMART6000 diffractometer was

through NSF-MRI grant (CHE-0215950). We would like to thank Drs. Larry Sallans and Stephen Macha for assistance with MS measurements.

Appendix A. Supplementary material

CCDC-1035784-1035786 contains the supplementary crystallographic data for this paper. These data can be obtained free of charge from The Cambridge Crystallographic Data Centre via www.ccdc.cam.ac.uk/data_request/cif

Appendix B. Supplementary data

Supplementary data related to this article can be found at <http://dx.doi.org/10.1016/j.jorganchem.2015.03.002>.

References

- [1] M. Albrecht, G. van Koten, *Angew. Chem. Int. Ed.* 40 (2001) 3750–3781.
- [2] M.E. van der Boom, D. Milstein, *Chem. Rev.* 103 (2003) 1759–1792.
- [3] D. Morales-Morales, *Mini-Rev. Org. Chem.* 5 (2008) 141–152.
- [4] J.M. Serrano-Becerra, D. Morales-Morales, *Curr. Org. Synth.* 6 (2009) 169–192.
- [5] D.M. Grove, G. Van Koten, A.H.M. Verschuuren, *J. Mol. Catal.* 45 (1988) 169–174.
- [6] W.D. Jones, in: D. Morales-Morales, C. Jensen (Eds.), *The Chemistry of Pincer Compounds*, Elsevier Science B.V., Amsterdam, 2007, pp. 441–444. Chapter 19.
- [7] S. Chakraborty, J. Zhang, J.A. Krause, H. Guan, *J. Am. Chem. Soc.* 132 (2010) 8872–8873.
- [8] S. Chakraborty, Y.J. Patel, J.A. Krause, H. Guan, *Polyhedron* 32 (2012) 30–34.
- [9] S. Chakraborty, J. Zhang, Y.J. Patel, J.A. Krause, H. Guan, *Inorg. Chem.* 52 (2012) 37–47.
- [10] S. Chakraborty, J.A. Krause, H. Guan, *Organometallics* 28 (2009) 582–586.
- [11] P. Bhattacharya, J.A. Krause, H. Guan, *Organometallics* 30 (2011) 4720–4729.
- [12] V. Pandarus, D. Zargarian, *Organometallics* (2007) 978–980.
- [13] J. Aydin, J.M. Larsson, N. Selander, K.J. Szabo, *Org. Lett.* 11 (2009) 2852–2854.
- [14] W.H. Bernskoetter, S.K. Hanson, S.K. Buzak, Z. Davis, P.S. White, R. Swartz, K.I. Goldberg, M. Brookhart, *J. Am. Chem. Soc.* 131 (2009) 8603–8613.
- [15] H. Salem, L.J.W. Shimon, Y. Diskin-Posner, G. Leitun, Y. Ben-David, D. Milstein, *Organometallics* 28 (2009) 4791–4806.
- [16] S. Kundu, W.W. Brennessel, W.D. Jones, *Inorg. Chem.* 50 (2011) 9443–9453.
- [17] D.M. Spasyuk, D. Zargarian, A. van der Est, *Organometallics* 28 (2009) 6531–6540.
- [18] J.-F. Gong, Y.-H. Zhang, M.-P. Song, C. Xu, *Organometallics* 26 (2007) 6487–6492.
- [19] Y. Motoyama, K. Shimozono, H. Nishiyama, *Inorg. Chim. Acta* 359 (2006) 1725–1730.
- [20] M. Gandelman, A. Vignalok, L.J.W. Shimon, D. Milstein, *Organometallics* 16 (1997) 3981–3986.
- [21] W. Sotoyama, T. Satoh, H. Sato, A. Matsuura, N. Sawatari, *J. Phys. Chem. A* 109 (2005) 9760–9766.
- [22] S.J. Farley, D.L. Rochester, A.L. Thompson, J.A.K. Howard, J.A.G. Williams, *Inorg. Chem.* 44 (2005) 9690–9703.
- [23] J.A.G. Williams, A. Beeby, E.S. Davies, J.A. Weinstein, C. Wilson, *Inorg. Chem.* 42 (2003) 8609–8611.
- [24] O.A. Blackburn, B.J. Coe, M. Helliwell, J. Raftery, *Organometallics* 31 (2012) 5307–5320.
- [25] G.D. Batema, K.T.L. van de Westelaken, J. Guerra, M. Lutz, A.L. Spek, C.A. van Walree, C. de Mello Donegá, A. Meijerink, G.P.M. van Klink, G. van Koten, *Eur. J. Inorg. Chem.* 2007 (2007) 1422–1435.
- [26] S. Tastan, J.A. Krause, W.B. Connick, *Inorg. Chim. Acta* 359 (2006) 1889–1898.
- [27] H. Jude, J.A. Krause Bauer, W.B. Connick, *Inorg. Chem.* 44 (2005) 1211–1220.
- [28] H. Jude, J.A. Krause Bauer, W.B. Connick, *Inorg. Chem.* 43 (2004) 725–733.
- [29] H. Jude, J.A. Krause Bauer, W.B. Connick, *Inorg. Chem.* 41 (2002) 2275–2281.
- [30] L.A. van de Kuil, H. Luitjes, D.M. Grove, J.W. Zwikker, J.G.M. van der Linden, A.M. Roelofsens, L.W. Jenneskens, W. Drenth, G. van Koten, *Organometallics* 13 (1994) 468–477.
- [31] L.-L. Shi, Y. Liao, G.-C. Yang, Z.-M. Su, S.-S. Zhao, *Inorg. Chem.* 47 (2008) 2347–2355.
- [32] D.M. Spasyuk, S.I. Gorelsky, A. van der Est, D. Zargarian, *Inorg. Chem.* 50 (2011) 2661–2674.
- [33] A.B. Salah, D. Zargarian, *Dalton Trans.* 40 (2011) 8977–8985.
- [34] W.J. Cherwinski, B.F.G. Johnson, J. Lewis, *J. Chem. Soc. Dalton Trans.* (1974) 1405–1409.
- [35] K. Moseley, P.M. Maitlis, *Chem. Commun.* (1971) 982–983.
- [36] J.A.M. van Beek, G. van Koten, G.P.C.M. Dekker, E. Wissing, M.C. Zoutberg, C.H. Stam, *J. Organomet. Chem.* 394 (1990) 659–678.
- [37] M. Albrecht, P. Dani, M. Lutz, A.L. Spek, G. van Koten, *J. Am. Chem. Soc.* 122 (2000) 11822–11833.

- [38] C.J. Moulton, B.L. Shaw, *J. Chem. Soc. Dalton Trans.* 1976 (1976) 1020–1024.
- [39] Z. Wang, S. Sugiarti, C.M. Morales, C.M. Jensen, D. Morales-Morales, *Inorg. Chim. Acta* 359 (2006) 1923–1928.
- [40] M.A. Bennett, H. Jin, A.C. Willis, *J. Organomet. Chem.* 451 (1993) 249–256.
- [41] H. Rimml, L.M. Venanzi, *J. Organomet. Chem.* 259 (1983) C6–C7.
- [42] M. Albrecht, R.A. Gossage, M. Lutz, A.L. Spek, G. van Koten, *Chem. Eur. J.* 6 (2000) 1431–1445.
- [43] W.R. Mason, H.B. Gray, *J. Am. Chem. Soc.* 90 (1968) 5721–5729.
- [44] D.A. Roberts, W.R. Mason, G.L. Geoffroy, *Inorg. Chem.* 20 (1981) 789–796.
- [45] A. Merle, M. Dartiguena Ve, Y. Dartiguenave, *J. Mol. Struct.* 13 (1972) 413–433.
- [46] L.L. Costanzo, S. Giuffrida, R. Romeo, *Inorg. Chim. Acta* 38 (1980) 31–35.